



# **Solving non-hydrostatic Navier-Stokes equations with a free surface**

J.-M. Hervouet

*Laboratoire National d'Hydraulique et Environnement,  
Electricité De France, Research & Development Division, France.*

## **Abstract**

This paper deals with the numerical solution of 3-dimensional Navier-Stokes equations with a free surface, in the framework of finite elements. The hydrostatic assumption is not done but the algorithm is built as an extension of an already existing hydrostatic Navier-Stokes solver. The results prove the robustness of the approach and show that the full 3D free surface Navier-Stokes equations are now a viable option against simplified forms like Boussinesq equations.

## **1 Introduction**

The hydroinformatic system Telemac, based on Finite Element techniques, addresses free surface and underground flows. In its present development stage, the system includes the Saint-Venant or shallow water equations (Telemac-2D), Navier-Stokes equations in 3 dimensions with a free surface (Telemac-3D), and also mild slope equations, wave action equations, water quality models, sediment transport equations in 2D and 3D, Richard's equations in 2D and 3D. Recent advances have led to a robust algorithm for the treatment of full non-hydrostatic 3D Navier-Stokes equations with a free surface, which allows rapid flows, hydraulic jumps, wetting and drying, so that a first result on the computation of a dam-break floodwave has been obtained and is presented here.

## **2 Overview of the method**

In Telemac-3D the space discretization is done with layers of vertical prisms formed by superimposed meshes of triangles. To overcome the problems of free

#### 4 Coastal Engineering VI

surface movements, the equations can be solved in a  $\sigma$ -transformed mesh, where the vertical coordinate varies in the range  $[0,1]$ , but this is not done for all steps. In the basic version, the pressure is hydrostatic and the free surface is computed by solving equations similar to the shallow-water equations. This basic hydrostatic version is briefly described hereafter, and will be used also with the non hydrostatic option.

##### Hydrostatic option:

The equations read:

Continuity:

$$\text{div}(\vec{U}) = 0 \quad (1)$$

Momentum:

$$\frac{\partial U}{\partial t} + \vec{U} \cdot \text{grad}(U) = -\frac{1}{\rho_0} \frac{\partial p_h}{\partial x} + \text{div}(v_t \text{grad}(U)) + f_x \quad (2)$$

$$\frac{\partial V}{\partial t} + \vec{U} \cdot \text{grad}(V) = -\frac{1}{\rho_0} \frac{\partial p_h}{\partial y} + \text{div}(v_t \text{grad}(V)) + f_y \quad (3)$$

Where  $p_h$  is the hydrostatic pressure,  $\rho_0$  is the reference density,  $v_t$  the turbulent viscosity, and  $f_x$  and  $f_y$  are source terms such as the Coriolis force.  $U$ ,  $V$ , and  $W$  are the Cartesian velocity components of the velocity  $\vec{U}$ .

According to the hydrostatic assumption, the hydrostatic pressure is written:

$$p_h = \rho_0 g (Z_s - z) + \rho_0 g \int_z^{Z_s} \frac{\Delta \rho}{\rho_0} dz \quad (4)$$

where  $\rho$  is the density,  $g$  the gravity acceleration,  $Z_s$  is the free surface elevation and the second term takes into account the buoyancy effects due to temperature or salinity.  $\Delta \rho$  is  $\rho - \rho_0$ .

Using an operator splitting approach, the solution procedure contains three steps: advection, diffusion, and free surface-continuity-pressure step. The last step looks formally like Shallow Water Equations in which depth-averaged values of the horizontal velocity field are used. This is where the pressure terms are treated in the form of the free-surface gradient. As a matter of fact, if  $U^{n+1}$  and  $V^{n+1}$  are the final horizontal components of velocity at the end of the time step, and  $U_D$  and  $V_D$  are the horizontal velocities after the diffusion step, we have to solve:

$$\frac{U^{n+1} - U_D}{\Delta t} = -g \frac{\partial Z_s}{\partial x} \quad \text{and} \quad \frac{V^{n+1} - V_D}{\Delta t} = -g \frac{\partial Z_s}{\partial y} \quad (5)$$

If we depth-average these equations, it yields:

$$\frac{u^{n+1} - \overline{U}_D}{\Delta t} = -g \frac{\partial Z_s}{\partial x} \quad \text{and} \quad \frac{v^{n+1} - \overline{V}_D}{\Delta t} = -g \frac{\partial Z_s}{\partial y} \quad (6)$$

where  $u^{n+1}$  and  $v^{n+1}$  are the final depth averaged velocities and the bar expresses the depth-average operator. This system can be considered as Shallow Water momentum equations without advection, friction nor diffusion, and can be solved by a Shallow Water Equations solver as Telemac-2D. The depth averaged continuity equation is also solved concurrently, and yields a new free surface. This equation is obtained without any approximation and is thus also valid in a 3D context. The 3D velocities are then easily retrieved because:

$$\frac{U^{n+1} - U_D}{\Delta t} = \frac{u^{n+1} - \overline{U}_D}{\Delta t} \quad \text{and} \quad \frac{V^{n+1} - V_D}{\Delta t} = \frac{v^{n+1} - \overline{V}_D}{\Delta t} \quad (7)$$

Finally, the vertical velocity  $W$  is obtained from the 3-dimensional continuity equation. This last step is one of the weakness of the hydrostatic solvers, the horizontal velocities are left unchanged and only the vertical velocity is modified to ensure a divergence free field. Errors on the horizontal velocity field will thus end up in wrong vertical velocities. This will not be the case with the non-hydrostatic option.

#### Non-hydrostatic option:

The basic idea of the method is a decomposition of the pressure into the hydrostatic pressure  $p_h$  and the hydrodynamic pressure denoted  $\pi$ :  $p = p_h + \pi$ . In the first phase only the hydrostatic pressure is taken into account as before, but an equation for  $W$  is added:

$$\frac{\partial W}{\partial t} + \vec{U} \cdot \text{grad}(W) = -\frac{1}{\rho_0} \frac{\partial \pi}{\partial z} + \text{div}(\mathbf{v}, \text{grad}(W)) \quad (8)$$

In the next step the hydrodynamic pressure is taken into account to ensure the continuity equation and yield a divergence free velocity field, this is a classical projection algorithm for Navier-Stokes equations. Namely, taking  $U_D$  and  $V_D$  as in the hydrostatic option, we now solve:

$$\frac{\vec{U}^{n+1} - \vec{U}_D}{\Delta t} = -\frac{1}{\rho_0} \overrightarrow{\text{grad}}(\pi) \quad (9)$$

and given the fact that  $\text{div}(\vec{U}^{n+1}) = 0$ , it yields:

$$\text{div}(\vec{U}_D) = \text{div}\left(\frac{\Delta t}{\rho_0} \overrightarrow{\text{grad}}(\pi)\right) \quad (10)$$

which is a well known Poisson equation. Once this equation is solved, the final velocity field is given by eqn (9).

Finally, the free surface is updated again with the help of the depth-averaged continuity equation, where the velocity is known and the depth  $h^{n+1}$  at time  $t^{n+1}$  is the unknown.



### 3 Results and applications

The applications that will be presented here are a solitary wave, a flow over a weir with a transcritical flow and a hydraulic jump caused by outflow boundary conditions, the mixing of two fluids of different densities, and the Malpasset dam-break.

#### 3.1 Solitary wave

This case is used to compare Boussinesq and Navier-Stokes solvers. A series of tests has been performed with a solitary wave in a 600 m long rectangular channel, with flat bottom. The depth is 10 m and the wave height is 2 m. It is well known that the hydrostatic assumption is not applicable for describing such a wave. Either Shallow Water equations or hydrostatic 3D Navier-Stokes equations lead to an artificial breaking. The solitary wave must propagate without changing its shape and celerity, yielding an ideal case for a model verification with a clear criterion. We have chosen for the initial condition the second approximation to a solitary wave given by Laitone in 1960 (ref. [4]). As the initial wave extends from  $-\infty$  to  $+\infty$ , the position of the maximum was chosen sufficiently far (80 m) from the boundary behind the wave. The non-hydrostatic option yields a behaviour of the wave comparable, though better in the wake, with what is obtained with a Boussinesq solver. For both models the time step is 0.1 s and the duration is 40 s. Figure 1 displays the vertical cross-section of the rectangular channel, with the solitary wave at different time steps. This result has been obtained using the 3D model with only 3 levels on the vertical, i.e. two layers of prisms. Computer time is only 60% of what is required with our Boussinesq solver. Table 1 summarises the computational times obtained with different equations and different number of levels in the case of 3D. Times are given for a HP C3700 workstation (785 MHz). The number of triangles in the mesh is 7206, the number of prisms in the 3D case with 11 levels is thus for example 72060.

Equations	Computer time
Shallow Water Equations (not relevant to the case)	72 s
Boussinesq	589 s
3D hydrostatic 11 levels (not relevant to the case)	382 s
3D non hydrostatic 11 levels	981 s
3D non hydrostatic 6 levels	483 s
3D non hydrostatic 3 levels	358 s
3D non hydrostatic 2 levels	249 s

Table 1: computational time of different equations

Shallow Water Equations and 3D hydrostatic are given in the table for comparison but are of course not relevant to the case of a solitary wave. They both give the same free surface elevation, which tends to a breaking of the solitary wave. The effect of adding the Boussinesq terms in the Shallow Water Equations is tremendous and the computer time rises from 72 s to 589 s. Compared to this result, the 3D computation appears to be more attractive up to 6 levels on the vertical. Actually the result is excellent as soon as at least 3 levels are used. The main time-consuming difficulties are, on Navier-Stokes side, the Poisson Pressure Equation, on Boussinesq side, the Helmholtz-like equations stemming from the extra terms added by Boussinesq in the Saint-Venant equations. In both cases matrices of the linear systems are mostly Laplacian matrices, which explains the same order of difficulties.

### 3.2 Flow over a weir

Figure 2 displays vertical cross-sections in the longitudinal axis of a 21 m long channel, with a flat bottom (elevation  $-0.2$  m) except between the abscissae  $x=7.12$  m and  $12.88$  m where the elevation is  $-0.0246875(x-10)^2$ . The width is 2 m and the discharge is  $2$  m<sup>3</sup>/s. A depth of 0.6 m is maintained downstream. A Manning friction coefficient of 0.025 is applied. The 2D mesh is shown at the top of the figure and the 3D mesh is composed of 6 superimposed 2D meshes. The free surface obtained is compared with an exact solution of Shallow Water Equations. Then, the velocity field, and the dynamic pressure are displayed. From upstream to downstream, the flow is successively fluvial, then critical, then supercritical, and after a hydraulic jump fluvial again. The bump of the free surface after the hydraulic jump is more realistic than what is given by the hydrostatic assumption of Shallow Water Equations.

### 3.3 Mixing of two fluids

Also known as the “lock exchange test-case”, the intrusion of a salt water wedge into a fresh water channel, after opening a lock gate, is a well known test-case. Applying the hydrostatic assumption for a gravitational current yields a wrong solution. The case is schematised as follows: two fluids with different densities are confined in a rectangular basin with impermeable walls and, at the initial time, an horizontal free surface. The left part of the basin is filled by the fluid of higher density. An interfacial wave is created and the denser fluid propagates on the right, along the bottom. The hydrostatic solution shows a rectangular pattern which is not observed in experiments, be it in nature or in laboratories. The non-hydrostatic solution is validated by numerous measurements (see e.g. Yih 1980). Figure 3 compares the hydrostatic (above) and non-hydrostatic (below) results. The density difference is obtained with a salinity of 1 g/l for the denser fluid (on the left) and 0 g/l for the other. The much better results of the non-hydrostatic

## 8 Coastal Engineering VI

version open the possibility of refined flow modelling in the field of 3-dimensional thermal plumes, or in salt-wedge studies in estuaries.

### 3.4 Malpasset dam-break

The 2-dimensional numerical simulation with Shallow Water Equations of a real dam-break which occurred in France in December 1959 has been extensively described in the first paper of reference [1]: A high resolution 2D dam-break model using parallelization. After recent advances in the treatment of tidal flats and dry zones in Telemac-3D, it is now possible to deal with such a case in 3D, and compute the solution of full 3D non-hydrostatic Navier-Stokes equations. Meshes with 2, 3, 4, 5, 6 and 7 levels of 2D meshes on the vertical have been tried. The inundation extent obtained with 4 levels is plotted on figure 4 and compared to the Saint-Venant solution. It is found that in this case there are only minor differences with a hydrostatic solution. Again as soon as at least 3 levels are used, there is no significant differences in the results.

## Conclusion

Robust 3D non-hydrostatic Navier-Stokes solvers with a free surface are now available for a wide range of applications including waves, wetting and drying, density effects, supercritical flows and hydraulic jumps. Such solvers will eventually replace Boussinesq solvers in a near future. It seems now reasonable to concentrate the efforts on the full Navier-Stokes equations, rather than trying to improve and optimize simplified forms. Further improvements are still necessary to deal with strong stratifications, and the sigma transformation should be suppressed, as it brings artificial diffusion effects. Unstructured meshes on the vertical, e.g. with tetrahedrons, would also allow a better local treatment of outfalls.

## References

- [1] Hydrological Processes, Volume 14, issue n°13. Special issue : the Telemac modelling system. Guest editors J.-M. Hervouet and P. Bates.
- [2] Hervouet J.-M., van Haren L. 1996. Recent advances in numerical methods for fluid flows. Chapter 6 of "Floodplain processes" Editors Anderson, Walling & Bates. Wiley & sons 1996.
- [3] Jankowski Jacek A., A non-hydrostatic model for free surface flows. Institut für Strömungsmechanik und Elektron. Rechnen im Bauwesen der Universität Hannover. Bericht Nr.56/1998.
- [4] Laitone E., The second approximation to cnoidal and solitary waves. Journal of Fluid Mechanics, 9, 430-444.1960
- [5] Yih C.-S., Stratified flows. *Academic press, London, New-York. 1980.*

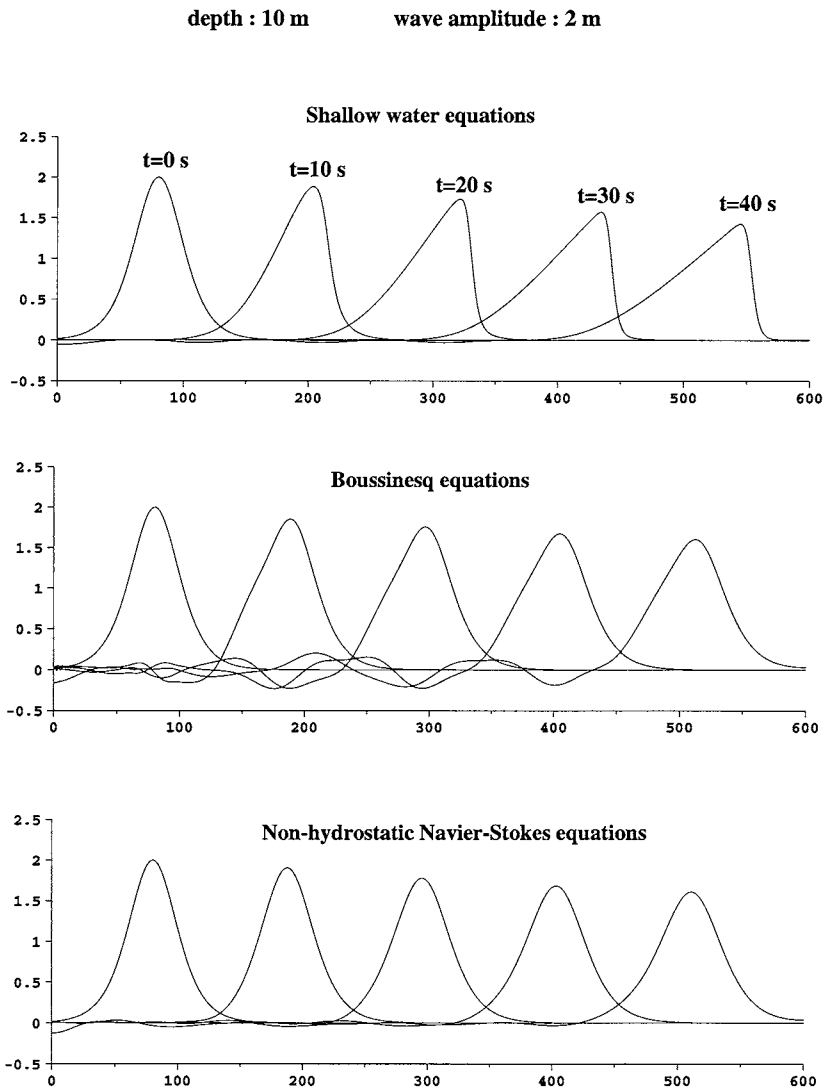


Figure 1: Solitary wave in a channel at 5 successive times. Comparison of shallow water, Boussinesq and Navier-Stokes equations.



## 10 Coastal Engineering VI

### six 2-dimensional meshes on the vertical

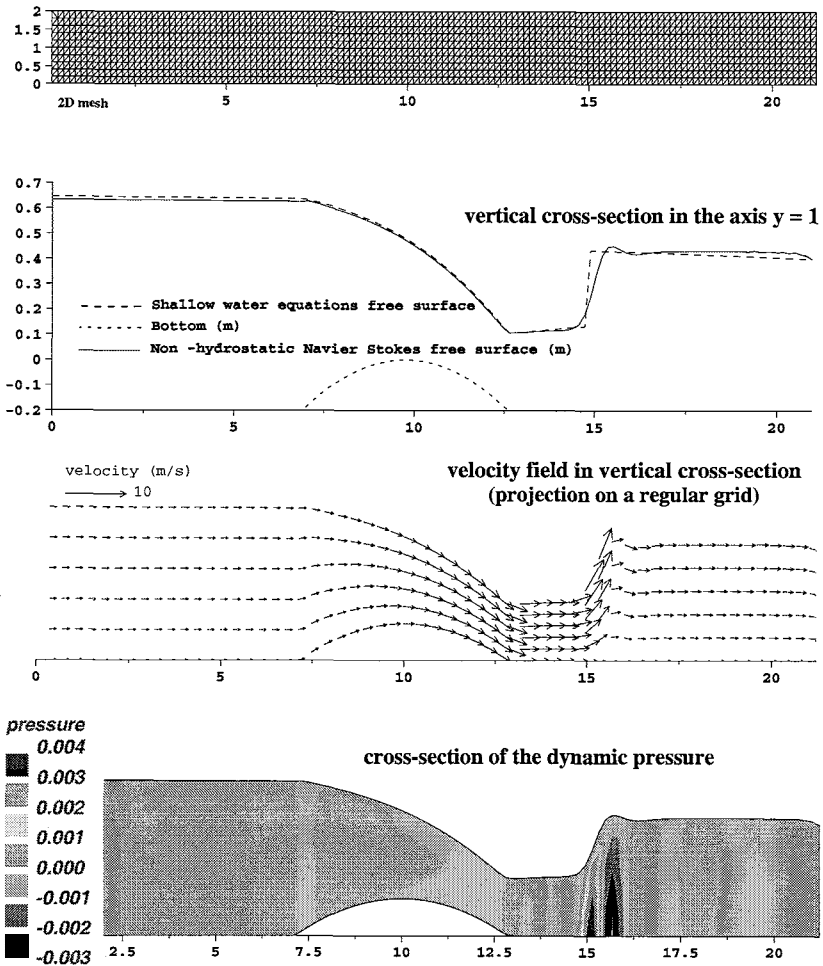


Figure 2: Non-hydrostatic Navier-Stokes solution of a flow on a weir, with a hydraulic jump.



### Vertical cross section in the axis of the channel

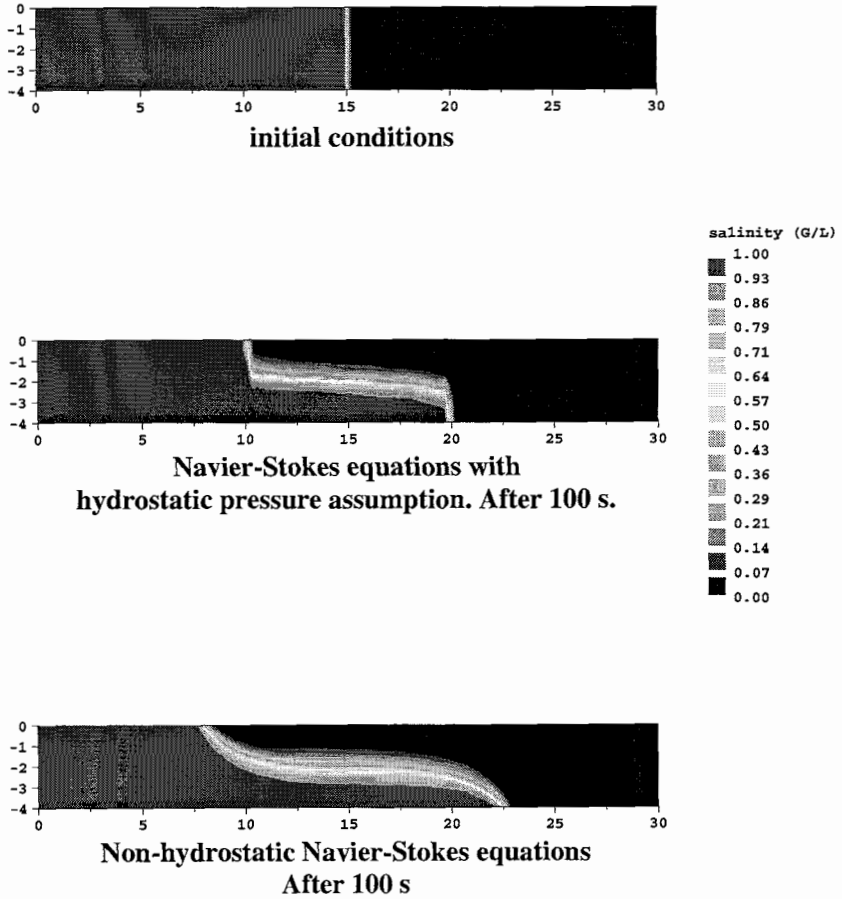


Figure 3: Mixing of 2 fluids, the lock exchange test-case. Comparison of hydrostatic and non hydrostatic solutions.



### Water depth 35 mn after the dam break

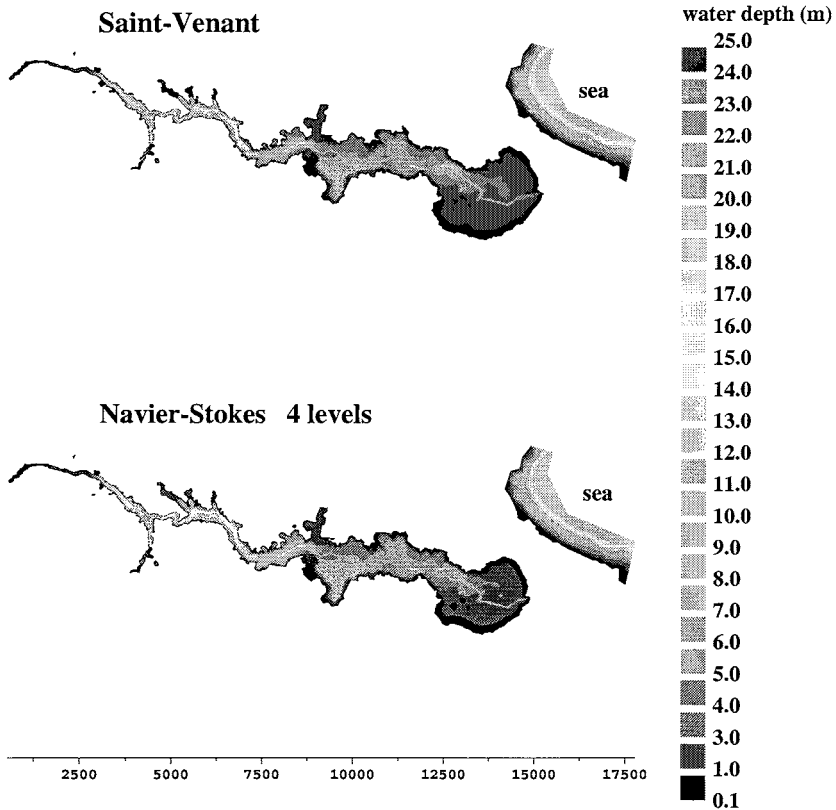


Figure 4: The Malpasset dam-break. Comparison of shallow water equations and Navier-Stokes equations.